Int. J. Electrochem. Sci., 17 **(2022)** Article Number: 220926, doi: 10.20964/2022.09.06

International Journal of
ELECTROCHEMICAL
SCIENCE
www.electrochemsci.org

Mini review

Electrochemical aptamer-based sensors for the detection of heavy metals

Shupan Ge[1,2,3] and Xiaohua Ma[1,2,]*

[1] Henan Key Laboratory of Biomolecular Recognition and Sensing, Shangqiu Normal University, Shangqiu, Henan, 476000, People's Republic of China
[2] Nanchang Vocational University, Nanchang, Jiangxi, 330000, People's Republic of China
[3] Guangxi Investment Group Laibin Electric Power Company Limited, Laibin, Guangxi, 546138, People's Republic of China
[*]E-mail: maxhsqnu@aliyun.com

Received: 22 May 2022 / *Accepted:* 14 June 2022 / *Published:* 7 August 2022

Heavy metal contamination has attracted extensive attention because of its threat to ecosystem and human health. It is highly desired to develop sensitive and selective methods for real-time detection of heavy metals because of the limitations and shortcomings of traditional detection techniques. Electrochemical aptamer-based sensors (aptasensors) have the advantages of high sensitivity and specificity and rapid response. This review discussed the basic principle and application of electrochemical aptasensors for the detection of heavy metals, including the labeled and label-free strategies.

Keywords: Electrochemical sensors; aptamers; heavy metals; signal label; label-free strategy

1. INTRODUCTION

With the acceleration of industrialization, heavy metal contamination is becoming more and more serious, such as Pb, As, Co, Ni, Cd, Hg, Au and Ag [1]. Most of the heavy metals are not necessary for life activities and will endanger human health. They can form the metal complexes when binding with the ligands containing N, S and O, thus changing the molecular structure of proteins and resulting in the inactivation of proteins or enzymes. Therefore, it is particularly important to develop simple, efficient, sensitive and selective methods for the detection of various heavy metals.

Traditional methods used for the detection of heavy metals include atomic absorption spectrophotometry, atomic fluorescence spectrometry, inductively coupled plasma spectrometry and X-ray spectrometry [2]. Although these methods have the advantages of high sensitivity and good

reproducibility, the sample pretreatment is usually complex, which often refers to concentration and extraction to suppressing the interference of other ions. Moreover, they require large and expensive instruments, professional operators, and long detection time. Compared with these methods, electrochemical analysis has the advantages of fast response, high sensitivity and low cost. In the presence of heavy metals, the change of current, electrochemical impedance or capacitance can be readily monitored. However, the specificity of electrochemical detection of metal ions is usually limited. Thus, the sensing electrodes are usually modified with specific materials to improve the electrochemical performances and detection specificity. Aptamers are a type of nucleic acids with specific binding ability to the targets [3]. They are usually single stranded DNA (dsDNA) or RNA fragments found by in vitro screening technology. Aptamers can bind with the target molecules with high affinity through electrostatic interaction, hydrogen bond, hydrophobic accumulation or van der Waals force under appropriate environment. Combined with the pairing effect of some complementary bases in the chain, aptamers can be adaptively folded into a stable secondary structure, such as hairpin, stem loop, G-quadruplex and T-junction. Therefore, aptamers have highly specific recognition ability to the target molecules. In addition, the synthesis of aptamers is simple, rapid and low-cost. It can specifically bind with a variety of targets such as biological small molecules, proteins, peptides, organics and metal ions. Electrochemical aptamer-based sensors (aptasensors) for the detection of heavy metals show better specificity and higher sensitivity than simple electrochemical technology [4]. They can be divided into labeled and labeled-free types according to the way of generating electrochemical signals. In the labeled electrochemical aptasensors, aptamers can be modified with redox-active molecules, nanomaterials and DNAzymes. In this work, we summarized the progress in the design of electrochemical aptasensors for the detection of heavy metals.

2. LABEL-FREE ELECTROCHEMICAL APTASENSORS

The specific recognition between aptamer and target can lead to the configuration change of aptamer, thus causing the direct or indirect signal change on electrode interface. The signal change can be detected by different electrochemical techniques. For example, Pb^{2+} can induce its aptamer to form a stable G-quadruplex structure; Gao et al. reported a label-free electrochemical aptasensor the sensitive detection of Pb^{2+} based on the π-π stacking interaction between graphene and the base units in DNA [5]. Graphene could be attached on the surface of DNA aptamer-modified electrode through the π-π stacking interaction, and then thionine molecules were assembled on the graphene surface to produce an obvious electrochemical signal. In the presence of Pb^{2+}, the structure of ssDNA on the electrode surface changed into G-quadruplex, which destroyed the interaction between the base units and graphene, thus reducing the amount of graphene and thionine adsorbed on the electrode surface and leading to the decrease of redox signal. Under the optimum experimental conditions, the peak current showed a linear relationship to the logarithm of Pb^{2+} concentration in the range of 1.6×10^{-13} to 1.6×10^{-10} mol/L, and a detection limit of 3.2×10^{-14} mol/L was attained. Cui et al. reported a label-free electrochemical aptasensor for sensitive determination of arsenite [6]. The aptamer was self-assembled on screen-printed carbon electrode through Au-S interaction. The negatively charged aptamer can adsorb cationic polydiallyl dimethyl ammonium (PDDA) through electrostatic interaction and thus repel other cationic species.

After the formation of aptamer/arsenite complex, the conformation of aptamer changed, resulting in the release of PDDA and facilitating the adsorption of $[Ru(NH_3)_6]^{3+}$. The target-induced conformational change can be used for sensitive and selective determination of arsenite with a range of 0.2 ~ 100 nM and a minimum detection concentration of 0.15 nM.

Gold nanoparticles (AuNPs) are widely employed to modify the electrode to accelerate the electron transfer and catalyze the redox reaction [7]. Moreover, AuNPs with a large specific surface area can provided and rich active sites to immobilize various biological molecules and maintain their biological activity. Zhao et al. reported a label-free and reusable electrochemical aptasensor based on the Pb^{2+}-induced formation of G-quadruplex [8]. Firstly, AuNPs were deposited on the surface of glassy carbon electrode by electrochemical reduction and further modified with ssDNA. The double-stranded structure formed by the hybridization of aptamer and ssDNA modified on the electrode surface has a large amount of negative charges, which hindered the redox reaction of negatively charged $[Fe(CN)_6]^{3-/4-}$ on the electrode surface and induced the increase of charge transfer resistance (R_{ct}). After the addition of Pb^{2+}, the formed G-quadruplex was separated from the electrode surface, which resulted in the decrease of surface negative charge and the reduction of R_{ct}. The linear range of the method is 0.001 ~ 100 μg/L and the detection limit is 0.0046 nM. Moreover, Tang et al. designed an electrochemical aptasensor for label-free detection of Pb^{2+} based on G-quadruplex [9]. In this method, gold nanoparticles (AuNPs) coated with polyionic oligonucleotides were modified on the gold electrode as signal amplification probes to provide high-density negative charges. In the presence of Pb^{2+}, the formation of G-quadruplex induced by Pb^{2+} reduced the negative charge on the electrode surface, thus allowing for the high selective detection of Pb^{2+}. The detection range of the sensor is 10^{-11} ~ 10^{-6} M and the detection limit is 8.5 pM.

Pb^{2+} can break the dsDNA formed between the aptamer and its complementary sequence. Jin et al. established an electrochemical aptasensor for the detection of Pb^{2+} based on catalytic hairpin assembly technology and porous carbon (PCs)-loaded platinum nanoparticles (PtNPs) as signal amplification units [10]. The released complementary DNA was then hybridized with the hairpin DNA on the electrode surface to trigger the catalytic hairpin assembly reaction, resulting in the attachment of a large number of biotin-labeled DNA stands on the electrode surface. Finally, a large number of platinum nanoparticles loaded on streptavidin-modified porous carbons (PCs) were captured by the electrode. A strong electrochemical signal was produced by the catalytic reaction of hydroquinone/H_2O_2 system. Zhuo et al. reported a ratiometric aptasensor for Pb^{2+} detection based on a novel electrochemiluminescence resonance energy transfer (ECL-RET) system from $O_2/S_2O_8^{2-}$ to the amino-terminated perylene derivative (PTC-NH_2) [11]. As shown in Figure 1, the glassy carbon electrode (GCE) was coated with gold-nanoparticles-functionalized fullerene nanocomposites (AuNPs@nano-C_{60}) and then was modified with thiol-labeled assistant probes (APs). After the hybridization between APs and capture probes (the aptamer of the Pb^{2+}, CPs), a large number of PTC-NH_2 could be intercalated into grooves of DNA duplexes formed on the electrode surface through the electrostatic interaction. Two ECL signal peaks at −0.7 V and −2.0 V were recorded, attributing to the emittance of PTC-NH_2 ($^1(NH_2{-}PTC)^2$*) and $O_2/S_2O_8^{2-}$ ($^1(O_2)_2$*), respectively. However, in the presence of Pb^{2+}, the higher affinity between Pb^{2+} and CPs facilitate the generation of the stable Pb^{2+} G-quadruplex structure and broke the dsDNA structure, leading to the release of PTC-NH_2 from the

electrode surface. Therefore, the ECL signal from $^1(NH_2{-}PTC)^{2*}$ reduced and the ECL signal from $^1(O_2)_2{}^*$ was increased. Finally, Pb^{2+} was sensitively detected in the range of 1.0×10^{-12} M to 1.0×10^{-7} M with a detection limit of 3.5×10^{-13} M.

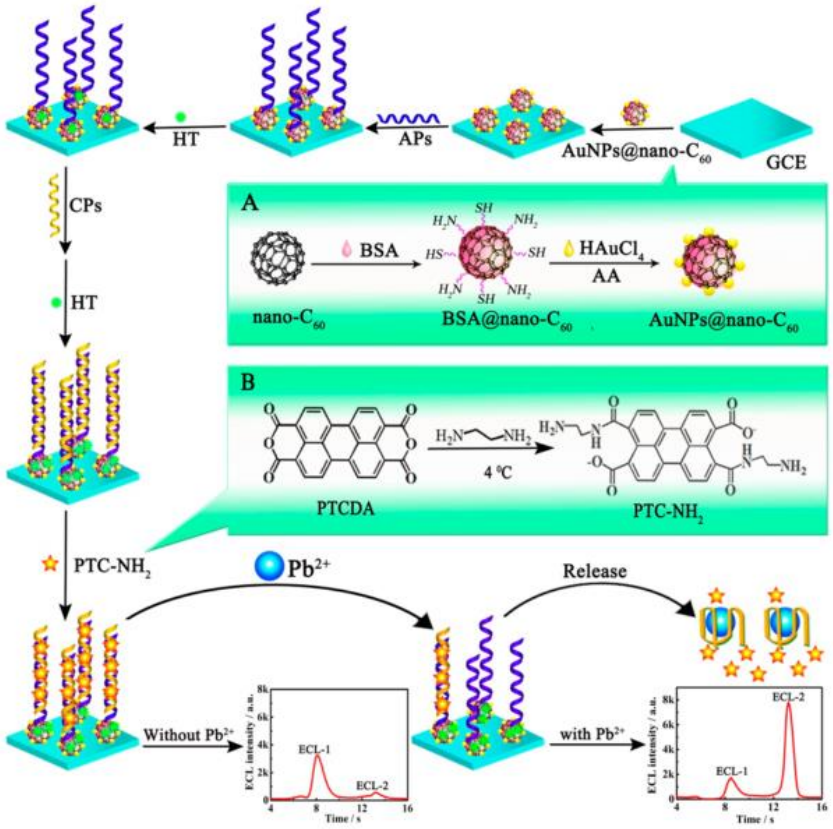

Figure 1. Schematic illustration of the preparation process of the ratiometric aptasensor: Inset of (A) and (B) display the preparation procedure of AuNPs@Nano-C_{60} and PTC-NH_2. Copyright 2015 American Chemical Society [11].

As a poisonous and widely distributed element in the environment, As(III) has been recognized as a threat to human health. Gu et al. established an electrochemical aptasensor for the detection of As(III) based on the hybrid chain reaction and exonuclease-assisted catalytic cascade reaction [12]. The aptamer and ssDNA were assembled on the surface of gold electrode to produce a large R_{ct}. In the presence of As(III), the aptamer specifically bound to As(III), resulting in the dissociation of its complementary DNA and the occurrence of catalytic cascade reaction. This led to the release of a large amount of DNA on the electrode surface, significantly reducing the R_{ct}. The detection limit of the aptasensor is as low as 0.02 ppb. Baghbaderani and Noorbakhsh constructed a label-free impedance aptasensor for high sensitive determination of As(III) with chitosan/Nafion-coated conductive surface platform and the signal amplification of carbon nanotubes [13]. The glass carbon electrode modified by chitosan/Nafion has high electron transfer kinetics and has the advantages of good reproducibility and selectivity, free medium and renewable biosensor interface. Ensafi et al. designed an aptasensor using 3D rGO-modified AuNPs for the determination of arsenite [14]. The thiolated aptamer was modified on the surface of rGO-AuNPs by the formation of Au-S bond. As(III) bound with the aptamer to cause the

formation of G-quadruplex complex, which hindered electron transfer and increased R_{ct} value. The detection limit of the aptasensor for As(III) is down to 1.4×10^7 μg/L and the linear range varied from 3.8×10^7 to 3.0×10^4 μg/L.

As one of the most poisonous heavy metals, Cd^{2+} can cause organ injuries and serious health risks. Because of its electrochemical property, Cd^{2+} can be directly determined by voltammetry. Wang et al. constructed an aptasensor for the detection of Cd^{2+} using reduced graphene oxide (rGO)/graphite carbon nitride (g-C_3N_4)-modified electrode [15]. As displayed in Figure 2, the rGO)/ g-C_3N_4 (GCN) was applied to modify the electode. Plentifulyy amino funtional groups in GCN could provide active site for the immoblization of aptamers. After the capture of Cd^{2+} in solution, the concenration of Cd^{2+} was determined by differential anodic stripping voltammetry (DPASV). The rGO significantly improved the conductivity and enhanced the electrochemical signal of Cd^{2+} captured by the aptamer. The sensor exhibited a linear range of 1 nM to 1 μM and a detection limit of 0.337 nM. Rabai et al. reported the electrochemical detection of Cd^{2+} by using the nanocomposites of gold nanoparticles (AuNPs), carbon nanotubes (CNTs) and chitosan (CS) to immobilize the Cd^{2+} aptamer [16]. The linear concentration range is 10^{-13} ~ 10^{-14} M and the detection limit is 0.02 pM. The sensor show good selectivity towards to other metal ions such as Pb^{2+}, Hg^{2+} and Zn^{2+}. Chen et al. constructed a signal-switching ratio electrochemical sensor based on partial complementary aptamer for the detection of Cd^{2+} [17]. AuNPs were electrochemically deposited on SPE for the immobilization of aptamer by the Au-S interaction. The other part of ssDNA semi-complementary to the aptamer could bind to electroactive Polythionine-Au (PTh-Au) at the 5'-terminal to form ssDNA@PTh-Au. The ssDNA@PTh-Au was then captured by the electrode through the hybridization with the aptamer on AuNPs-modified electrode. The interaction between Cd^{2+} and aptamer led to the release of ssDNA@PTh-Au. The signals were recorded by the response of Cd^{2+} and PTH-Au. The linear concentration range of this method for Cd^{2+} detection is 2×10^{-3} ~ 8×10^{-1} mg/L with a detection limit of 7×10^{-4} mg/L.

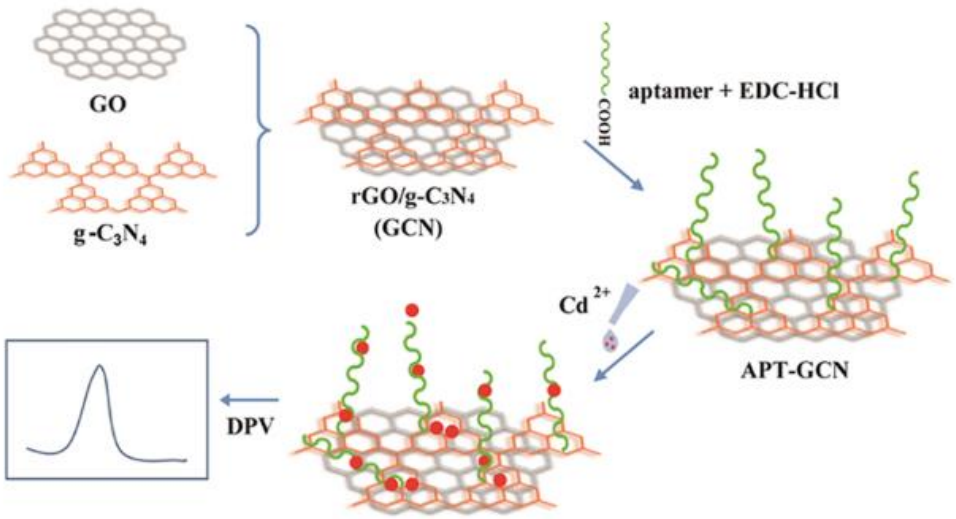

Figure 2. Schematic illustration of the fabrication of the APT-GCN aptasensor and its detection of the cadmium cation [15]. Copyright 2018 American Chemical Society.

Graphene with single-layer sheet structure is composed of carbon atoms. Hydrophobic and π-π stacking interactions can occur between graphene and the base units of nucleic acid. GO nanosheets can effectively bind with ssDNA and prevent the dissociation of ssDNA from the surface of graphene. Wang et al. developed an electrochemical aptasensor for Hg^{2+} detection based on the ultrahigh electron transfer ability of graphene and its unique interaction with ssDNA [18]. As shown in Figure 3, graphene adsorbed by ATP or Hg^{2+} aptamer on Au electrode through the strong π–π interaction could cause a remarkable decrease of R_{ct}. In the presence of target (ATP or Hg^{2+}), the binding of aptamer and the target blocked the adsorption of graphene, which led to the increase of R_{ct}.

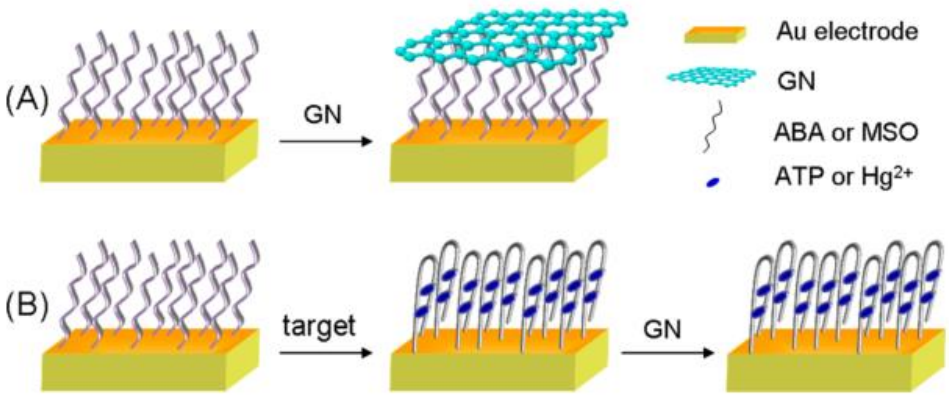

Figure 3. Electrochemical sensing strategy for the detection of ATP or H^{2+}: (A) GN was adsorbed on ABA/Au electrode due to the strong π–π interaction, and a large R_{ct} decrease was obtained. (B) In the presence of ATP, ATP binding aptamer (ABA) bound ATP and formed duplex which could not adsorb GN and resulted in a small R_{ct} decrease [18]. Copyright 2012 American Chemical Society.

Moreover, Deng et al. constructed an electrochemical aptasensor for highly sensitive detection of Pb^{2+} by combining the guanine (G)-rich aptamer with gate-controlled signal amplification [19]. After binding with Pb^{2+}, the G-rich aptamer was folded to form a G-quadruple structure (G4-Pb^{2+}) than could cover the channel of redox probe on the electrode surface, thus forming a gate-controlled effect and causing the decrease in the redox current. This effect can be used for the quantitative detection of Pb^{2+} with a linear range of $1 \times 10^{-13} \sim 5 \times 10^{-11}$ mol/L. The detection limit is 3.6×10^{-14} mol/L. Ma et al. reported a controlled release system electrochemical aptasensor (CRSEA) for supersensitive determination of Hg^{2+} (Figure 4) [20]. In this study, mesoporous silica nanoparticles (MSNs) were utilized as containers to load toluidine blue (TB) molecules and AuNPs-linked specific ssDNA (Au NP-sssDNA) were employed as a molecular gate. In the presence of Hg^{2+}, T-rich ssDNA was transformed into the hairpin structure via the coordination between T and Hg^{2+}, resulting in the release of AuNP-ssDNA from the MSNs. The TB molecules released from MSNs could be detected by differential pulse voltammetry (DPV) to indirectly monitor the concentration of Hg^{2+}. This method exhibited a wide linear range from 10 pM to 100μM and a low LOD of 2.9 pM.

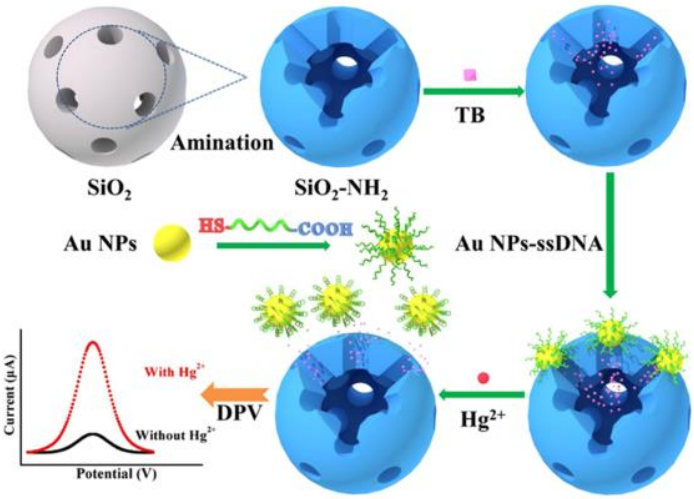

Figure 4. Schematic representation of the electrochemical controlled release aptasensor for Hg^{2+} [20]. Copyright 2020 American Chemical Society.

3. LABELED ELECTROCHEMICAL APTASENSORS

3.1 Electroactive labels

With the increasing maturity of molecular labeling technology, the labeled aptamers have widely been used for the design of electrochemical sensors with improving sensitivity. Although the label-free electrochemical sensor has the advantages of simplicity and low cost, it faces the disadvantages of low sensitivity and poor selectivity. With the improvement of synthetic methods, signal molecules with redox activity or catalytic activity can be modified to DNA by physical adsorption, covalent coupling, avidin-biotin interaction and other means, such as ferrocene (Fc) and methylene blue (MB). The target can be quantified by the change of electrochemical signal caused by the target-aptamer binding.

The specific interaction between the target and the aptamer or DNA can induce the change of DNA conformation, thus changing the distance between the marker and the electrode surface. This is closely related to the change in the electrochemical signal intensity. Zhuang et al. reported an electrochemical sensor for Hg^{2+} detection by the target-induced change in the hairpin structure of DNA [21]. The hairpin DNA modified with ferrocene was assembled onto the electrode surface through the formation of Au-S bond, in which ferrocene is far away from the electrode. The strong coordination of thymine–Hg^{2+}–thymine opened the hairpin structure, causing the ferrocene group to approach the electrode and the increase in the redox current. The sensor has good repeatability and linear range ($5.0 \times 10^{-9} \sim 1.0 \times 10^{-6}$ mol/L) and low detection limit (2.5×10^{-9} mol/L). With the same principle, there are many reports on the detection of heavy metal ions. For example, Wen et al. reported the detection of arsenite using MB-labeled ssDNA based on the conformational change [22]. The designed sensors have good selectivity and sensitivity, and the aptamer has being optimized to shorten the length. Moreover, Wu et al. reported a Hg^{2+} electrochemical aptasensor by modifying ferrocene at the end of DNA [23]. The complementary DNA strand was fixed on the electrode through Au-S interaction. In the presence of Hg^{2+}, the two DNA strands were hybridized each other, and ferrocene group was close to the electrode

to produce a strong electrochemical signal. The binding of Hg^{2+} to DNA resulted in the separation of the two strands. The ferrocene group was far away from the electrode, and the electrochemical signal was weakened. The detection limit of the electrochemical sensor is 6.0×10^{-11} mol/L.

rGO can not only improve the electron transfer, but also adsorb ssDNA via π-π stacking interaction when it is utilized to modify the electrode. Yu et al. constructed an ultrasensitive electrochemical sensor for the detection of Pb^{2+} based on the different affinity of ssDNA and G-quadruplex to rGO [24]. The MB-labeled aptamers were adsorbed on the surface of rGO-modified glassy carbon electrode through π-π stacking interaction, resulting in a strong electrochemical signal. In the presence of Pb^{2+}, the aptamer in single chain state was transformed into G-quadruplex structure and then separated from the surface of rGO, thus leading to the decrease in the redox current of MB. The detection limit of the sensor for Pb^{2+} is 0.51 fM. Based on the hairpin structure of gold nanoparticles (AuNPs), thionine and aptamer complementary chain, Taghdisi et al. constructed an electrochemical aptasensor for ultrasensitive and selective detection of Pb^{2+} (Table 1) [25]. In the presence of Pb^{2+}, the aptamer formed a hairpin structure and the electrochemical signal is low. In the absence of Pb^{2+}, thionine-AuNPs were combined with the aptamer to produce a strong electrochemical signal. The electrochemical aptasensor can determine Pb^{2+} in water and milk, and the detection limits are 326 and 537 pM, respectively.

Hg^{2+} can specifically bind with two T residues of DNA to form T-Hg^{2+}-T complex. Ali et al. reported the detection of Hg^{2+} and Pb^{2+} by modifying their aptamers with different electroactive molecules [26]. The aptamer of Hg^{2+} formed a hairpin structure by the T-Hg^{2+}-T interaction. The aptamer of Pb^{2+} formed a G-quadruplex structure by the G-Pb^{2+}-G interaction. In both cases, the electroactive molecules were closer to the electrode surface, which enhanced the electron transfer efficiency and the current value. The detection limit of this method is 0.1 ng/mL.

The interaction between the target and the aptamer can unzip the dsDNA containing an aptamer sequence. By modifying the DNA strand with electroactive molecules, electrochemical aptasensors have been widely developed for metal ion detection. For example, Yuan et al. reported an electrochemical aptasensor for simultaneously identifying and determining Pb^{2+} and Cd^{2+} in fruits and vegetables [27]. Aptamers labeled with different electroactive molecules (methylene blue and ferrocene) were fixed on the surface of gold electrode for hybridization with the complementary DNA to produce strong electrochemical signals. The specific binding between the metal ions and the aptamers destroyed the double chain structure, which made the electroactive molecule-labeled aptamers be separated from the electrode, thus weakening the electrochemical signal. The linear range of this method for simultaneous determination of Pb^{2+} and Cd^{2+} is 0.1 ~ 1000 nM. The detection limits for Pb^{2+} and Cd^{2+} are 89.31 and 16.44 pM, respectively. Moreover, Yuan et al. designed an electrochemical aptasensor for Cd^{2+} detection using ferrocene-modified aptamer [28]. The complementary chain of aptamer was self-assembled on the electrode surface for hybridization with the aptamer. Cd^{2+} competed with the complementary chain to bind the aptamer, making the ferrocene-modified aptamer fall off from the electrode surface and causing the decrease in the electrochemical signal of ferrocene. Lee et al. reported a signal-enhanced electrochemical aptasensor for the detection of Cd^{2+} [29]. The dsDNA formed by methylene blue-labeled aptamer and its partial complementary DNA was adsorbed on the surface of rGO-modified electrode. The rigid double chain structure made methylene blue far away from the electrode and hindered the

electron transfer, resulting in low oxidation current of methylene blue. When Cd^{2+} bound to the aptamer, the double chain structure was destroyed, which made methylene blue close to the electrode surface and caused the increase in the current intensity. The sensor has a linear range of 1 fM to 1 nM with a detection limit of 0.65 fM. Recently, Wu et al. reported a electrochemical Au(III) aptasensor with high sensitivity and tunable dynamic range [30]. As presented in Figure 5, MB-labeled DNA probes was designed with 6 (A6) and 12 (A12) consecutive adenines, respectively. The complex formed between Au(III) and the adenine bases in probes could rigidify the corresponding DNA probe, thereby inhibiting the access of MB to the electrode surface and decreasing the current intensity. Through the choice of different DNA probes, Au(III) was determined within in a tunable dynamic range and a detection limit of 50 and 20 nM for the A6 and A12 aptasensors.

In addition to covalent modification, electroactive molecules can be adsorbed to DNA by electrostatic interaction or embedded in grooves between dsDNA. Wen et al. designed a sensitive and label-free electrochemical aptasensor based on the conformational change of ssDNA induced by arsenite [22]. The dsDNA on the electrode surface can adsorb a large amount of methylene blue and produce a strong electrochemical signal. Arsenite selectively bound to the aptamer to destroy the dsDNA, making the aptamer be dissociated from the electrode to the solution. Therefore, the total amount of methylene blue on the modified electrode decreased with the decrease in the peak current.

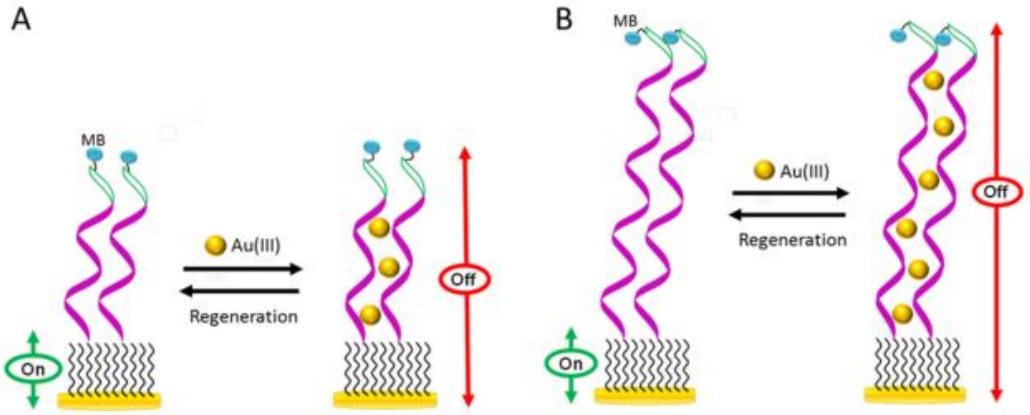

Figure 5. Signaling mechanism of the A6 (A) and A12 (B) E-ION Au(III) sensors [30]. Copyright 2016 American Chemical Society.

3.2 Nanomaterial labels

Nanomaterials with a unit size in the range of 1-100 nm have attracted extensive attention by virtue of their unique surface effect, thermal conductivity and optical property. Nanoparticles have the characteristics of easy synthesis, small particle size, large specific area and high surface free energy, which improved the sensitivity of heavy metal detection. According to the types of nanomaterials, nanoparticle labels for heavy metal ion detection can be divided into AuNPs and quantum dots (QDs). AuNPs have good biocompatibility, high electron density, dielectric properties, fluorescence quenching effect, photothermal conversion, surface enhanced Raman scattering effect and surface plasmon resonance effect [7]. These advantages make them be widely used as the electrode materials or signal

labels of electrochemical sensors for disease diagnosis, biological and food safety monitoring and heavy metal ion detection (Table 1). AuNPs have been widely used to modify the electrode in order to improve the electron transfer rate and electrode area for aptamer immobilization, so as to achieve the effect of signal amplification. Liu et al. established an electrochemical sensor based on T-Hg^{2+}-T structure to detect Hg^{2+} [31]. Through layer-by-layer assembly technology, AuNPs and chitosan were modified on glassy carbon electrode for the immobilization of ferrocene-labeled aptamer. The aptamer was recognized by Hg^{2+} to fold into a hairpin structure, resulting in ferrocene group close to the electrode surface. The logarithm of Hg^{2+} concentration has a good linear relationship with the DPV peak current in the range of 0.01 ~ 500 nM. The detection limit of the sensor is 5 pM. Yadav et al. reported an electrochemical aptasensor based on aptamer and Ag/Au alloy nanoparticles to detect As(III). After As(III) was captured by the aptamer, Ag/Au alloy nanoparticles promoted the electrochemical reduction reaction of As(III) and significantly enhanced the reduction current [32]. The detection limit of the sensor is 3 pg/L. They also constructed an electrochemical aptasensor using Ag/Au alloy nanoparticles to modify the glassy carbon electrode [33]. The specific binding of Pb^{2+} and aptamer formed a G-quadruplex structure and enhanced the electrochemical signal. The detection limit measured by CV and DPV is 0.03×10^{-2} μg/L and the detection limit measured by EIS is 0.04×10^{-2} μg/L.

Table 1. Analytical performances of nanomaterials-based electrochemical aptasensors for the detection heavy metal ions.

Electrode Modifier	Metal ions	Detection limit	Linear range	Ref.
AuNPs	Pb^{2+}	149 pM	0.7 ~ 300 nM	[34]
AgPtNPs	Pb^{2+}	32 fM	0.1 pM ~ 100 pM	[35]
graphene	Hg^{2+}	0.12 nM	0.5 ~ 100 nM	[36]
rGO	Hg^{2+}	0.16 fM	0.1 fM~100 nM	[37]
SWNTs	Pb^{2+}	0.41 nM	1 ~10 nM	[38]
graphene/AuNPs	Pb^{2+}	0.001 aM	1 aM~100 nM	[39]
Fe_3O_4/rGO	Hg^{2+}	30 pM	0.1~100 nM	[40]

AuNPs are also often used to modify other carbon materials to further improve conductivity. For example, Mushiana et al. reported an electrochemical aptasensor for arsenite detection based on the composites of carbon nanoparticles and AuNPs [41]. The specific binding between aptamer and arsenite changed the configuration of aptamer, which was conducive to the electron transfer of redox probe and resulted in the enhancement of voltammetric signal. The detection limit of the sensor is 0.092 ppb. Wang et al. developed a reusable electrochemical sensor based on thymine (T)-modified AuNPs/rGO composites for the detection of Hg^{2+} [42]. The T bases on the electrode surface allowed for the capture of Hg^{2+} through T-Hg^{2+}-T coordination. The AuNPs/rGO nanocomposites significantly enhanced the dissolution peak current of Hg^{2+}. Finally, the detection range of the sensor is 5.0×10^{-11} ~ 5.0×10^{-6} mol/L with a detection limit as low as 7.0×10^{-12} mol/L. Ding et al. reported an electrochemical aptasensor to detect Pb^{2+} [43]. The screen-printed carbon electrode was modified by the composite of AuNPs and polypyrrole (gold@ppy) to amplify the current signal. The dsDNA was immobilized on the

electrode to bind with Pb^{2+}. In the presence of Pb^{2+}, the G-rich aptamer on the electrode surface formed a G-quadruplex, leading to an increase in the peak current. The linear range of the method is 0.5 ~ 10 nM and the detection limit is 0.36 nM. In addition, Zhang et al. developed an electrochemical sensor to detect Ag^+ [44], in which the free ssDNA on AuNPs could form a stable cytosine-Ag^+-cytosine (C-Ag^+-C) complex. A large number of C-Ag^+-C facilitated the formation of silver nanoclusters through electrochemical reduction, thus obtaining a stripping voltammetry signal. AuNPs could accelerate silver stripping, so as to amplify the electrical signal for measuring the Ag^+ concentration.

In addition to being used as the substrate modification materials, AuNPs can also be used as the markers to enhance the electrochemical signals. Taghdisi et al. designed an electrochemical aptasensor using exonuclease III and AuNPs [34]. In the absence of Pb^{2+}, the aptamer was hybridized with the complementary hairpin DNA on the electrode surface, and the formed dsDNA was sheared by exo III. The released aptamer caused more hairpin DNA sequences to be cut. Finally, the ssDNA remained on the electrode surface could adsorb a large number of AuNPs to enhance the electrochemical signal of redox probe. On the contrary, in the presence of Pb^{2+}, the aptamer preferentially bound to Pb^{2+}. This prevented AuNPs from binding to the sensing electrode surface, resulting in a small peak current of redox probe. The detection limit of this method is 149 pM.

Aptamer can encircle around single-wall carbon nanotubes (SWCNTs) through π-π stacking and enhance the hydrophility and dispersion of SWCNTs in solution. Wang et al. constructed an electrochemical sensor for the detection of arsenite based on the interaction of aptamers and SWCNTs [45]. The ssDNA aptamer was adsorbed on the surface of SWCNTs through π-π stacking. Binding of arsenite to the G/T base of ssDNA reduced the π-π interaction between SWCNTs and ssDNA, resulting in the release of ssDNA from SWCNTs. The resulting SWCNTs were then adsorbed onto the self-assembled monolayer-modified gold electrode, greatly enhancing the electron transfer efficiency and producing a sensitive and specific response transduction signal. This signal was related to arsenite concentration. By monitoring the current mediated by SWCNTs, the linear detection concentration of arsenite is 0.5~10 μG/L with a detection limit down to 0.5 μg/L. Wen et al. reported the detection of arsenite based on GO-assisted production of Prussian blue nanoparticles (PBNPs) as the redox signal probes [46]. The thiolated aptamer was self-assembled on the surface of gold electrode through Au-S bond and GO was adsorbed through π-π stacking interaction, which promoted the formation of PBNPs on the surface of GO to produce an electroactive indicator in situ. Without arsenite, many GO/PBNPs are covered on the electrode surface to produce a strong electrochemical signal. In the presence of arsenite, the aptamer recognized arsenite to form a complex with a curly structure through hydrogen bonding, resulting in the reduction in the number of GO/PBNPs on the electrode surface and decrease in the redox signal. Finally, the linear range of the method is 0.2~500 μg/L, and detection limit is 58 ng/L.

Quantum dots (QDs) belong to semiconductor nanomaterials with composite or multilayer core-shell structures. They have unique optical and electrical properties, such as narrow size distribution, high quantization, size-dependent absorption and photoluminescence. QDs-labeled aptamers or target molecules have been used to design electrochemical sensors by measuring the content of heavy metals in QDs components. For example, Lu et al. reported an electrochemiluminescent sensor using CdSe QDs to label ssDNA [47]. DNA was assembled on the electrode through the Au-S bond, and then the terminal

amino at the labeled DNA was conjugated with the carboxylated CdSe QDs. In the presence of Pb^{2+}, the G-rich single chain was fold into G-quadruplex structure, which shortened the distance between QDs and electrode, thus reducing the electrochemiluminescence intensity. In the range of $1.0 \times 10^{-10} \sim 1.0 \times 10^{-8}$ mol/L, the concentration of Pb^{2+} is correlated with the electrochemiluminescence intensity. Zhao et al. developed a photoelectrochemical biosensor for the detection of Hg^{2+} based on dual signal amplification of exciton energy transfer (EET) and sensitization effect. As illustrated in Figure 6, the indium tin oxide (ITO) slice was decorated successively with TiO_2 NPs and CdS QDs. Probe DNA (pDNA) was bound on the electrode and was then labeled with Rh123. AuNP-labeled target DNA (Au-tDNA) was hybridized with pDNA and the photocurrent decreased because of the EET between CdS QDs and AuNP and the inhibited sensitization effect. In the presence of Hg^{2+}, the DNA duplexes were disrupted and the EET was hampered, leading to the recovery of the photocurrent. Meanwhile, the close of Rh123 to the electrode resulted in the formation of the sensitization structure. Finally, the biosensor showed a wide linear range (10 fM to 200 nM) and a low detection limit (3.3 fM) [48].

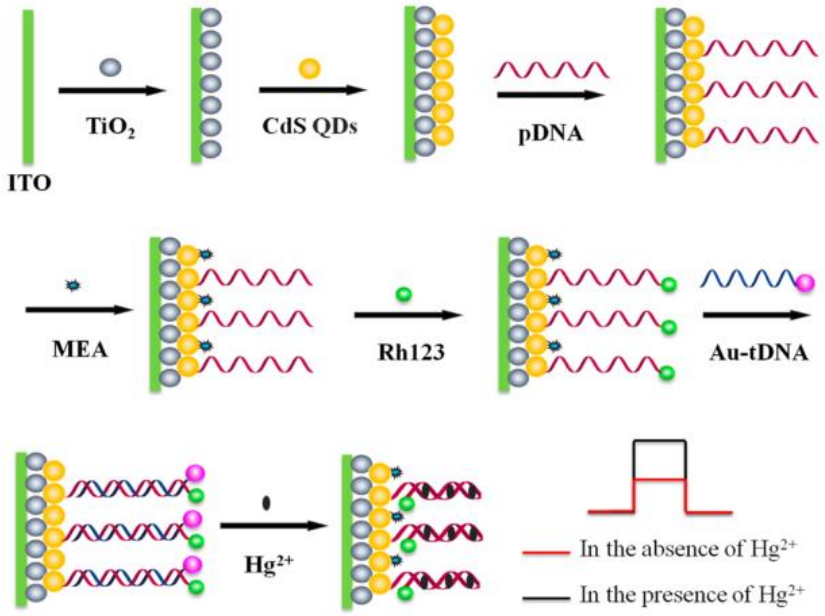

Figure 6. Fabrication procedure of the PEC biosensor for Hg^{2+} detection [48]. Copyright 2015 American Chemical Society.

Metal organic frameworks (MOFs), a class of porous crystalline materials, were composed of metal nodes and organic ligands. Besides their facinating properties of large suface area and tunable structures, MOFs can adsorb the negatively charged DNA through electrostatic and π-π stacking interactions. Zhang et al. designed a novel Fe(III)-based MOF (Fe-MOF) and mesoporous Fe_3O_4@C [49]. The core-shell nanostructured composites composed of nanocapsules were used to detect Pb^{2+} and As^{3+}. The composite could provide a large number of binding sites for aptamer. Metal ions induced the aptamer to form a G-quadruplex structure, which hindered the electron transfer. Finally, the detection limits of Pb^{2+} and As(III) were 2.27 and 6.73 pM, respectively. Based on the aptamer-based recognition and resistive pulse technology, Mayne et al. prepared an aptasensor for monitoring Pb^{2+} and Hg^{2+}[50].

When the aptamer-modified nanomaterials passed through the RP sensor, the change of charge state and density could be observed. The target binding led to the decrease of charge density.

Field effect transistors (FET) have been widely used in different fields, because of their ability to transduce recognition or binding events on the FET surface into electrical signals. An et al. developed a sensitive field effect transistor (FET) aptasensor using carboxylic polypyrrole (CPPy)-coated flower like MoS_2 nanospheres for in-situ determination of As(III) [51]. The nanospheres were successfully prepared by vapor deposition polymerization. Then, the aptamer-modified nanospheres were prepared into a liquid ion gated FET system to produce ultrafast response. The interaction between As(III) and aptamer produced a field induced current change, resulting in obvious resolution of As(III) at low concentration. The aptasensor can specifically recognize As(III) in the mixture.

3.3 DNAzyme labels

A variety of enzymes such as proteases, DNAzymes and RNases have been widely used as the labels to design different biosensors. DNAzymes are also used in the detection of heavy metals due to their high stability and strong recognition ability. However, the catalytic activity of a single DNAzyme is not high. Its activity would be activated when it is combined with cofactors such as nucleic acid, amino acid or metal ions. Based on the specificity of T-rich Hg^{2+} aptamer and the high catalytic activity of template deoxynucleotidyl transferase (TDT), Si et al. developed an electrochemical sensor for Hg^{2+} detection [52]. Template-independent TDT prolonged the aptamer end of 3'-OH by repeating bases. The extended product could capture many methylene blue-modified signal probes to the electrode surface and produced high-intensity electrochemical signals. However, in the presence of Hg^{2+}, the adapter would form a hairpin structure, which was not conducive to the catalytic extension of TDT enzyme and thus reduced the number of signal probes on the electrode surface. The detection limit of the sensor is 0.1 pM. Yang et al. reported the detection of Pb^{2+} with square wave voltammetry at DNAzyme/AuNPs/GO-modified electrode [53]. The thiol-modified guanine-rich DNA strands were self-assembled onto the AuNPs on the electrode surface through the formation of Au-S bonds. The aptamer could bind with Pb^{2+} to form a stable parallel G-quadruplex, which allowed for the binding of hemin to form DNAzyme with peroxidase activity. The formed DNAzyme catalyzed the electrochemical oxidation of hydroquinone (HQ) by H_2O_2, so as to amplify the electrochemical signal for highly sensitive detection of Pb^{2+}. The linear range is $5.0 \times 10^{-9} \sim 1.0 \times 10^{-6}$ mol/L. Based on the same principle, other heavy metal ions have been determined. Thus, this detection technology exhibits great potential in the detection of heavy metals.

4. CONCLUSION

In summary, the principle and application of electrochemical aptasensors for the detection of heavy metal ions have been discussed. Although aptamers have many advantages, there are still some challenges. For example, the interaction mechanism between metal ions and aptamers needs to be

profoundly studied and the chains of aptamers should be shortened to reduce the cost. Moreover, the reproducibility of aptasensors prepared in parallel with multiple electrodes should be further improved.

ACKOWLEDGMENTS
This work was supported by the Doctoral Research Foundation of Shangqiu Normal University (7001-700165).

References

1. L. Wang, X. Peng, H. Fu, C. Huang, Y. Li and Z. Liu, *Biosens. Bioelectron.*, 147 (2020) 111777.
2. M. R. Huang, G. L. Gu, F. Y. Shi and X. G. Li, *Chin. J. Anal. Chem.*, 40 (2012) 50.
3. A. B. Iliuk, L. Hu and W. A. Tao, *Anal. Chem.*, 83 (2011) 4440.
4. W. Guo, C. Zhang, T. Ma, X. Liu, Z. Chen, S. Li and Y. Deng, *J. Nanobiotechnology*, 19 (2021) 166.
5. F. Gao, C. Gao, S. He, Q. Wang and A. Wu, *Biosens. Bioelectron.*, 81 (2016) 15.
6. L. Cui, J. Wu and H. X. Ju, *Biosens. Bioelectron.* , 79 (2016) 861.
7. M. Negahdary, *Talanta*, 216 (2020) 120999.
8. G. Zhao, *Int. J. Electrochem. Sci.*, 16 (2021) 150956.
9. W. X. Tang, J. Yu, Z. Z. Wang, I. Jeerapan, L. Yin, F. Zhang and P. G. He, *Anal. Chim. Acta*, 1078 (2019) 53.
10. H. L. Jin, D. Zhang, Y. Liu and M. Wei, *RSC Adv.*, 10 (2020) 6647.
11. Y.-M. Lei, W.-X. Huang, M. Zhao, Y.-Q. Chai, R. Yuan and Y. Zhuo, *Anal. Chem.*, 87 (2015) 7787.
12. H. D. Gu, Y. Y. Yang, F. Chen, T. T. Liu, J. Jin, Y. Pan and P. Miao, *Chem. Eng. J.*, 353 (2018) 305.
13. S. S. Baghbaderani and A. Noorbakhsh, *Biosens. Bioelectron.*, 131 (2019) 1.
14. A. A. Ensafi, F. Akbarian, E. Heydari-Soureshjani and B. Rezaei, *Biosens. Bioelectron.*, 122 (2018) 25.
15. X. F. Wang, W. Y. Gao, W. Yan, P. Li, H. H. Zou, Z. X. Wei, W. J. Guan, Y. H. Ma, S. M. Wu, Y. Yu and K. J. Ding, *ACS Appl. Nano Mater.*, 1 (2018) 2341.
16. S. Rabai, A. Teniou, G. Catanante, M. Benounis, J. L. Marty and A. Rhouati, *Sensors*, 22 (2021) 105.
17. Z. Chen, C. Liu, X. Su, W. Zhang and X. Zou, *Sens. Actuat. B: Chem.*, 346 (2021) 130506.
18. L. Wang, M. Xu, L. Han, M. Zhou, C. Zhu and S. Dong, *Anal. Chem.*, 84 (2012) 7301.
19. H. Deng, M. Sun, X. Wei, H. Li and J. Li, *Chin. J. Anal. Chem.*, 44 (2016) 888.
20. N. Ma, X. Ren, H. Wang, X. Kuang, D. Fan, D. Wu and Q. Wei, *Anal. Chem.*, 92 (2020) 14069.
21. J. Zhuang, L. Fu, D. Tang, M. Xu, G. Chen and H. Yang, *Biosens. Bioelectron.*, 39 (2013) 315.
22. S. Wen, C. Zhang, R. Liang, B. Chi, Y. Yuan and J. Qiu, *Microchim. Acta*, 184 (2017) 4047.
23. D. Wu, Q. Zhang and H. Wang, *Biosens. Bioelectron.*, 25 (2010) 1025.
24. S. H. Yu, C. S. Lee and T. H. Kim, *Nanomaterials*, 9 (2019) 817.
25. S. M. Taghdisi, N. M. Danesh, P. Lavaee, M. Ramezani and K. Abnous, *Sens. Actuat. B: Chem.*, 234 (2016) 462.
26. M. H. Ali, M. E. Elsherbiny and M. Emara, *Int. J. Mol. Sci.*, 20 (2019) 2511.
27. M. Yuan, S. Qian, H. Cao, J. Yu, T. Ye, X. Wu, L. Chen and F. Xu, *Food Chem.*, 382 (2022) 132173.
28. M. Yuan, S.-Q. Qian, H. Cao, F. Xu, T. Ye, J.-S. Yu, W. Guo, J.-Y. Wu and A. Ti-kan, *Chin. J. Anal. Chem.*, 48 (2020) 1701.

29. C.-S. Lee, S. H. Yu and T. H. Kim, *Microchem. J.*, 159 (2020) 105372.
30. Y. Wu and R. Y. Lai, *Anal. Chem.*, 88 (2016) 2227.
31. Y. Liu, Y. Deng, T. Li, Z. Chen, H. Chen, S. Li and H. Liu, *J. Biomed. Nanotechnol.*, 14 (2018) 2156.
32. R. Yadav, V. Kushwah, M. S. Gaur, S. Bhadauria, A. N. Berlina, A. V. Zherdev and B. B. Dzantiev, *Int. J. Environ. Anal. Chem.*, 100 (2020) 623.
33. R. Yadav, A. N. Berlina, A. V. Zherdev, M. S. Gaur and B. B. Dzantiev, *SN Appl. Sci.*, 2 (2020) 2077.
34. S. M. Taghdisi, N. M. Danesh, M. Ramezani, M. Alibolandi and K. Abnous, *Microchim. Acta*, 184 (2017) 2783.
35. W. Xu, X. Zhou, J. Gao, S. Xue and J. Zhao, *Electrochim. Acta*, 251 (2017) 25.
36. Y. Zhang, J. Xie, Y. Liu, P. Pang, L. Feng, H. Wang, Z. Wu and W. Yang, *Electrochim. Acta*, 170 (2015) 210.
37. S. H. Yu and T. H. Kim, *J. Biomed. Nanotech.*, 15 (2019) 1824.
38. Y. Lian, M. Yuan and H. Zhao, *Fullerenes, Nanotub. Carbon Nanostruct.*, 22 (2014) 510.
39. Y. Zhang, G. M. Zeng, L. Tang, J. Chen, Y. Zhu, X. X. He and Y. He, *Anal. Chem.*, 87 (2015) 989.
40. J. Y. Luo, D. F. Jiang, T. Liu, J. M. Peng, Z. Y. Chu and W. Q. Jin, *Biosens. Bioelectron.*, 104 (2017) 1.
41. T. Mushiana, N. Mabuba, A. O. Idris, G. M. Peleyeju, B. O. Orimolade, D. Nkosi, R. F. Ajayi and O. A. Arotiba, *Sens. Bio-Sens. Res.*, 24 (2019) 100280.
42. N. Wang, M. Lin, H. Dai and H. Ma, *Biosens. Bioelectron.*, 79 (2016) 320.
43. J. N. Ding, D. W. Zhang, Y. Liu, M. L. Yu, X. J. Zhan, D. Zhang and P. Zhou, *Anal. Methods*, 11 (2019) 4274.
44. Y. Zhang, H. Li, J. Xie, M. Chen, D. Zhang, P. Pang, H. Wang, Z. Wu and W. Yang, *J. Electroanal. Chem.*, 785 (2017) 117.
45. Y. Wang, P. Wang, Y. Wang, X. He and K. Wang, *Talanta*, 141 (2015) 122.
46. S. Wen, Y. Wang, Y. Yuan, R. Liang and J. D. Qiu, *Anal. Chim. Acta.*, 1002 (2018) 82.
47. L. Lu, L. Guo, J. Li, T. Kang and S. Cheng, *Appl. Surf. Sci.*, 388 (2016) 431.
48. M. Zhao, G.-C. Fan, J.-J. Chen, J.-J. Shi and J.-J. Zhu, *Anal. Chem.*, 87 (2015) 12340.
49. Z. Zhang, H. Ji, Y. Song, S. Zhang, M. Wang, C. Jia, J. Tian, L. He, X. Zhang and C. Liu, *Biosens. Bioelectron.*, 94 (2017) 358.
50. L. Mayne, C. Y. Lin, S. D. R. Christie, Z. S. Siwy and M. Platt, *ACS Nano*, 12 (2018) 4844-4852.
51. J. H. An and J. Jang, *Nanoscale*, 9 (2017) 7483.
52. X. X. Si, S. Y. Tang, K. M. Wang, G. F. Zhou, J. J. Xia, Y. Zhao, H. Zhao, Q. P. Shen and Z. H. Liu, *Anal. Lett.*, 52 (2019) 2883.
53. R. Yang, T.-F. Kang, L.-P. Lu and Q. Ye, *Chin. J. Anal. Chem.*, 49 (2021) 309.